Check for updates

Circulation Research

ORIGINAL RESEARCH

Imaging of Existing and Newly Translated Proteins Elucidates Mechanisms of Sarcomere Turnover

Guy Douvdevany,* Itai Erlich,* Lilac Haimovich-Caspi, Tomer Mashiah, Maksymilian Prondzynski, Maria Rosaria Pricolo, Jorge Alegre-Cebollada, Wolfgang A. Linke, Lucie Carrier, Izhak Kehat

BACKGROUND: How the sarcomeric complex is continuously turned over in long-living cardiomyocytes is unclear. According to the prevailing model of sarcomere maintenance, sarcomeres are maintained by cytoplasmic soluble protein pools with free recycling between pools and sarcomeres.

METHODS: We imaged and quantified the turnover of expressed and endogenous sarcomeric proteins, including the giant protein titin, in cardiomyocytes in culture and in vivo, at the single cell and at the single sarcomere level using pulse-chase labeling of Halo-tagged proteins with covalent ligands.

RESULTS: We disprove the prevailing protein pool model and instead show an ordered mechanism in which only newly translated proteins enter the sarcomeric complex while older ones are removed and degraded. We also show that degradation is independent of protein age and that proteolytic extraction is a rate-limiting step in the turnover. We show that replacement of sarcomeric proteins occurs at a similar rate within cells and across the heart and is slower in adult cells.

CONCLUSIONS: Our findings establish a unidirectional replacement model for cardiac sarcomeres subunit replacement and identify their turnover principles.

GRAPHIC ABSTRACT: A graphic abstract is available for this article.

Key Words: cells, cultured ■ muscle proteins ■ myocytes, cardiac ■ proteostasis ■ sarcomeres

In This Issue, see p 471 | Meet the First Author, see p 472

Downloaded from http://ahajournals.org by on December 16, 2024

Almost all biological processes depend on the assembly of proteins into functional complexes. The protein subunits of these functional complexes must be continuously replaced since mammalian cells often live much longer than their proteins. Two models for the assembly of complexes were previously proposed. In the first model, the complex is in a dynamic equilibrium with a pool of cytoplasmic proteins and continuously recycles and exchanges subunits with the pool through de- and reassembly.[1] This exchange was shown to maintain simple complexes such as actin fibers and microtubules.[2,3] An alternative model proposes a sequential assembly,[4] where the complex is formed following an ordered series of steps. For example, the 26S proteasome shows a sequential assembly.[5] However, the mechanism by which such complexes are continuously maintained once they are fully assembled, and the role of subunit recycling in their maintenance remains largely unknown.[6]

The sarcomere is the basic contractile protein complex of striated muscle, including cardiomyocytes. It is composed of the contractile myofilament proteins myosin

Correspondence to: Izhak Kehat MD, PhD, The Ruth and Bruce Rappaport Faculty of Medicine, Technion - Israel Institute of Technology, Efron St, 9649 Bat Galim, Haifa 31096, Israel. Email ikehat@technion.ac.il
*G. Douvdevany and I. Erlich contributed equally.
Supplemental Material is available at https://www.ahajournals.org/doi/suppl/10.1161/CIRCRESAHA.123.323819.
For Sources of Funding and Disclosures, see page 486.
© 2024 American Heart Association, Inc.
Circulation Research is available at www.ahajournals.org/journal/res

Novelty and Significance

What Is Known?

- Cardiomyocytes live for many months and years, but sarcomeric proteins have short half-lives and must be continuously replaced.
- It has been proposed that replacement of sarcomeric proteins occurs by protein recycling between the sarcomeric structure and cytoplasmic pools.

What New Information Does This Article Contribute?

- Sarcomeric proteins are not recycled, and only newly translated proteins enter the sarcomeric structure.
- The degradation is independent of protein age, and proteolytic extraction determines the turnover rate.
- The turnover occurs at a similar rate across the cardiomyocytes and across the heart.
- The turnover of titin decreases with the maturation of cardiomyocytes and does not accelerate in hypertrophy.

Despite the longevity of cardiomyocytes, sarcomeric proteins have limited half-lives and require continuous replacement. Our study challenges the prevailing hypothesis that sarcomeric proteins can be recycled. Instead, we demonstrate that newly synthesized proteins integrate into the sarcomere, while older ones are removed and degraded. This degradation process is independent of protein age, with proteolytic extraction playing a major role in determining turnover rates. Across both cardiomyocytes and the heart, the replacement of sarcomeric proteins—such as titin—occurs at a similar rate, slowing down as cardiomyocytes mature and remaining unaffected by hypertrophy. This unidirectional replacement model provides important insights into how cardiac sarcomeres maintain their subunits, ensuring robust turnover throughout the heart.

Nonstandard Abbreviations and Acronyms

7BRO	7-bromoheptanol
AAV	adeno-associated virus
ALLN	N-acetyl-leucyl-leucyl-norleucinal
eGFP	enhanced green fluorescent protein
HITI	homology-independent targeted integration
JF-525	Janelia Fluor-525
JF-635	Janelia Fluor-635
MYL2	myosin regulatory light chain 2
MYOM1	M-line myomesin-1
NMVM	neonatal mice ventricular cardiomyocyte
NRVM	neonatal rat ventricular cardiomyocyte
PE	phenylephrine
TTN	titin
YFP	yellow fluorescent protein

and actin linked by TTN (titin), along with several other regulatory, structural, and accessory proteins.[7] Cardiomyocytes must continuously maintain their sarcomeres since sarcomeric proteins have a short half-life,[8] and the decreased sarcomere and sarcomeric protein content in failing hearts suggests that failure to do so may lead to heart failure.[9,10] According to the prevailing model of sarcomere maintenance, sarcomeres are maintained by cytoplasmic soluble protein pools with free recycling between pools and sarcomeres.[11–13] Support for this model came from fluorescence recovery after photobleaching experiments with fluorescently tagged sarcomeric proteins that show recovery of fluorescent-actin,[14,15] ACTN2 (α-actinin 2), telethonin, TPM1 (tropomyosin 1),[16] and TTN[17] after bleaching within several hours. In the latter study, it was even proposed that TTN molecules can move between adjacent sarcomeric complexes.[17]

Here, we developed a pulse-chase approach based on the covalent binding of different color fluorescent HaloTag ligands to image the replacement of older sarcomeric proteins by newly translated ones in cardiomyocytes in culture and in vivo. We imaged and measured the turnover of overexpressed and endogenous sarcomeric proteins, including the largest known protein TTN within the sarcomeric complex, in cultured cells and in vivo, at the single cell and the single sarcomere level. In contrast to the current protein pool model of sarcomere maintenance, our findings provide evidence for an ordered process in which newly translated proteins are continuously added to the complex while assembled proteins are continuously removed, degraded, and not recycled. We further show that once assembled, newly synthesized proteins are just as likely to be removed and degraded as older ones, and that proteolytic cleavage is needed for their extraction from the sarcomere. Our study thus establishes the unidirectional replacement model for cardiac sarcomeres.

METHODS

Data Availability

The data that support the findings of this study are available from the corresponding author upon reasonable request. The detailed methods section is available in the Supplemental Material.

Downloaded from http://ahajournals.org by on December 16, 2024

Animal Experiments

All animal procedures were approved by the Technion - Israel Institute of Technology Institutional Animal Care and Use Committee and conducted in accordance with guidelines for the care and use of laboratory animals. All results are reported in compliance with the Animal Research Reporting of In Vivo Experiments guidelines. Mice were randomly assigned to each experimental group by a coin toss.

RESULTS

Sarcomere Maintenance Is a Unidirectional Process

To image protein turnover in single living cardiomyocytes, we initially expressed Halo-tagged sarcomeric proteins in cultured neonatal rat ventricular cardiomyocytes (NRVMs) using adenoviral vectors. For the Z-line ACTN2 and the A-band MYL2 (myosin regulatory light chain 2) sarcomeric proteins, we used full-length sequences (ACTN2-Halo and Halo-MYL2), and for the large MYOM1 (M-line myomesin-1) and the A-band MYBPC3 (cardiac myosin-binding protein C), we used the N- and C-terminal fragments, respectively (MYOM1-Halo and Halo-MYBPC3). These fragments are sufficient for stable integration into sarcomeres.[18,19] After 48 hours, to allow expression of the Halo-tagged proteins, we pulsed the cells with the Oregon Green HaloTag ligand. HaloTag is a modified haloalkane dehalogenase that covalently and irreversibly binds to HaloTag ligand.[20] Therefore, once bound by the ligand, the existing Halo-tagged proteins in the cell remain permanently tagged with fluorescent green. To ensure that all the Halo-tagged proteins in the cell are bound by a ligand, we followed by pulsing with the nonfluorescent blocker ligand 7BRO (7-bromoheptanol) at a high concentration.[21] We then extensively washed the cells from excess ligands, photobleached a small area in the sarcomere, added the far-red HaloTag ligand JF-635 (Janelia Fluor-635), and imaged the cardiomyocytes for at least 72 hours (Figure 1A). We limited the frequency of imaging to 12 to 24 hours to reduce phototoxicity. The JF-635 ligand shows almost no light absorption in aqueous solution, but upon binding to HaloTag, it increases its absorbance and fluorescence by more than 100-fold and therefore can be used for continuous live cell imaging.[22] As expected, we did not observe a far-red fluorescence signal immediately after the addition of the JF-635 ligand, confirming that all the Halo-tagged proteins in the cell were already bound and that unbound JF-635 does not significantly fluoresce. However, once new Halo-tagged sarcomeric proteins were translated, their available HaloTag could bind the JF-635 ligand and display far-red fluorescence. Our approach therefore allowed us to follow 2 populations of sarcomeric proteins in the myocytes: older proteins labeled in green and newly translated sarcomeric proteins labeled in far-red. Over time, we observed an increase in the sarcomeric far-red fluorescence signal across the myocyte's sarcomeres along with a simultaneous decrease in green fluorescence, showing that newly synthesized proteins were added to the sarcomere and gradually replaced the older ones (Figure 1B).

We wondered whether subunit recycling is part of the maintenance process, and therefore we photobleached a small part of the green-labeled sarcomere at the beginning of the time lapse (Figure 1A and 1B). According to the protein pool model, sarcomeres would be maintained by a pool of cytoplasmic proteins containing a mixture of both older recycled and newly translated sarcomeric proteins. As a result, the photobleached sarcomeric proteins should be gradually replaced by both old green-labeled proteins and new far-red–labeled proteins from the pool (Figure S1). Contrary to this prediction, we found that the photobleached area gradually filled with new far-red–labeled proteins, whereas the green signal failed to recover, showing sarcomeric proteins are not recycled (Figure 1B). To test whether we could identify diffusion, we also expressed ACTN2-Halo and performed fluorescence recovery after photobleaching in rat fibroblasts. Green-labeled ACTN2-Halo fluorescence recovered in fibroblasts within a minute of bleaching (Figure S2), in contrast to cardiomyocytes, where no recovery occurred.

To quantify our findings and measure the intensity of the green and far-red signals, we stacked the time-lapse images, drew a linear region of interest along the myofibril, and calculated the median amplitude of the signal intensity over time in these 2 channels along the line (Figure S3). In addition to the sarcomeric signal, we also observed a nuclear accumulation of the signal for MYOM1, which likely represents an aggregate, and were therefore careful not to include the nucleus in our analyses. Assuming a first-order kinetic, we fitted an exponential decay function to the degradation, or a function that gives the difference between 1 and the exponential decay to fit to synthesis, and calculated the sarcomeric half-lives of proteins from the fitted curves (Figure 1C). These data show that the sarcomeric half-lives calculated for ACTN2, MYOM1, MYBPC3, and MYL2 were similar. Our approach does not require the assumption of a steady state for quantification, and we could calculate the half-life from either the degradation rate of green-labeled proteins or from the accumulation of far-red–tagged proteins. While these calculations yielded values in the same range, the half-lives calculated from accumulation were longer than those calculated from degradation. Some correction factor is likely to be required, and bleaching from the time-lapse imaging could have contributed to accelerating green fluorescence decline and delaying far-red fluorescence accumulation. Together, these analyses show that proteins are turned over in the sarcomere with a half-life of 20 to 42 hours in cultured cardiomyocytes.

Downloaded from http://ahajournals.org by on December 16, 2024

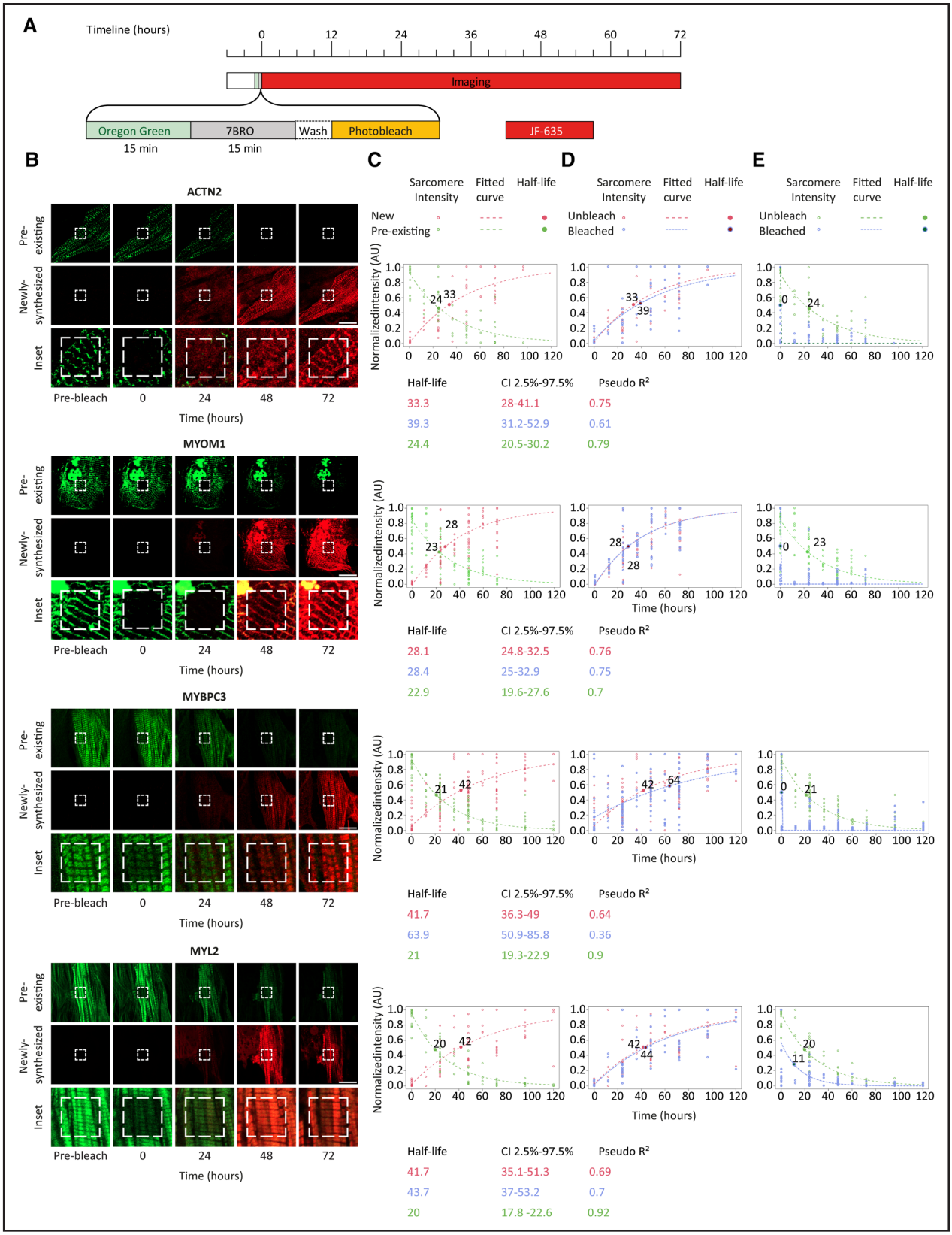

Figure 1. Imaging of sarcomere turnover shows a unidirectional process.

A, Pulse-chase experiment timeline: Cardiomyocytes expressing Halo-tagged sarcomeric proteins were incubated with Oregon Green ligand, followed by a nonfluorescent blocker ligand 7BRO (7-bromoheptanol), washed, and incubated with far-red JF-635 (Janelia Fluor-635) HaloTag ligand. A small square part of the cell was photobleached, followed by at least 72 hours of time-lapsed imaging. **B**, Representative time-lapse images of cardiomyocytes expressing Halo-tagged ACTN2, MYOM1, MYBPC3, and MYL2 in the green (top), far-red (middle), and (*Continued*)

Downloaded from http://ahajournals.org by on December 16, 2024

We measured and compared the increase in incorporation of newly translated far-red–labeled proteins outside and inside the bleached area and found similar rates, showing that sarcomeric proteins in different myofibrils are replaced simultaneously and at similar rates, and that our photobleaching did not damage the sarcomere (Figure 1D). Similarly, we measured and compared the changes in the existing, green-labeled protein signal outside and inside the bleached area (Figure 1E). All the proteins studied showed an exponential decline in intensity outside the bleached area, and for ACTN2, MYOM1, and MYBPC3, we did not observe any recovery of the green signal in the bleached area. The exception was a small resurgence of green fluorescence immediately after photobleaching for MYL2, followed by an exponential decay (Figure 1E), which may represent a small mobile, unincorporated pool of MYL2. However, even if such a MYL2 pool existed, it would be relatively small. Clearly, most of the existing MYL2 proteins in the sarcomere were replaced by newly synthesized ones and not through recycling. We could also quantify the turnover of single sarcomeres using super-resolution, showing the half-lives of individual sarcomeres within the same cell were similar (Figure S4). To further validate our half-life measurements, we performed similar experiments and analyzed them using SDS-PAGE with direct measurements of fluorescence from the gel. This analysis showed similar half-lives for ACTN2 (Figure S5A through S5C). The half-life of ACTN2 was also estimated following blockade of translation using cycloheximide for 8 hours in NRVMs, showing a similar half-life (Figure S5D and S5E).

Collectively, our data refute the prevailing protein pool hypothesis and prove that sarcomere maintenance is unidirectional: new proteins are incorporated into the sarcomere, but older proteins are extruded and degraded and cannot be recycled. Our measurements of the half-lives also imply that sarcomeric proteins are replaced at similar rates throughout the myocyte sarcomeres.

Imaging Turnover of Endogenous Sarcomeric Proteins

To confirm that our turnover model also applies to endogenous cardiac proteins, we used neonatal mice ventricular cardiomyocytes (NMVMs) derived from animals in which HaloTag was knocked-in to the I-band section of the largest known protein, the sarcomeric protein TTN.[23] We used the same protocol as used in NRVMs to image the turnover of endogenous TTN in NMVM. The preexisting TTN proteins were gradually and uniformly replaced by newly translated ones across the cardiomyocyte (Figure 2A). After photobleaching, there was no reemergence of the green fluorescence, showing that endogenous TTN cannot be recycled (Figure 2A). Quantification of our data showed that TTN is turned over with a half-life of about 15 to 31 hours (Figure 2B through 2D).

Next, we used the CRISPR/Cas9-based homology-independent targeted integration (HITI) strategy[24] to knock-in the HaloTag in the C terminus of the endogenous *Actn2* locus (Figure S6A). We isolated NMVMs from Cas9-expressing mice[25] and transduced them with adeno-associated viruses (AAVs) encoding for the donor cassette and for either the *Actn2* C-terminal single guide RNA or for control nontargeting single guide RNA. Strong Z-line staining was observed after the HaloTag ligand addition in ≈15% of cardiomyocytes only when *Actn2* single guide RNA was used, indicating that HaloTag cassette was integrated properly into the frame in these cardiomyocytes (Figure S6B and S6C). SDS-PAGE analysis confirmed the expression of ACTN2-Halo at the appropriate molecular weight, albeit with lower levels compared with adeno-virally overexpressed ACTN2-Halo (Figure S6D and S6E). We followed the turnover of endogenous ACTN2 with knocked-in HaloTag, showing that endogenous ACTN2 cannot be recycled (Figure 2E). Quantification of the data showed that endogenous ACTN2 is turned over with a half-life of about 19 to 31 hours (Figure 2F through 2H).

We also transduced NMVMs with adenoviral vectors encoding for ACTN2-Halo and compared the turnover rates of exogenously overexpressed ACTN2-Halo to endogenous HITI generated knock-in ACTN2-Halo (Figure 2I and 2J). We found that these turnover rates were similar, implying that expression level does not determine the turnover of sarcomeric proteins in the complex. We used the same HITI approach to knock-in Halo to the C terminus of endogenous *Myom1* and calculated the half-life, showing a similar value to that calculated with overexpressed N-terminal fragment of MYOM1 (Figure S6F and S6G). Here, we did not observe a nuclear accumulation, suggesting it resulted from either the expression of an N-terminal fragment or from the higher expression level achieved using adenoviral vectors.

Figure 1 Continued. the magnified merged channel (bottom) before the photobleaching, immediately after (0), and at 24, 48, and 72 hours, showing gradual replacement of preexisting proteins (green) with newly synthesized ones (far-red). The dashed white square is the photobleached field. It is gradually filling with new far-red–labeled proteins but not with green-labeled ones. Scale bar: 30 µm. **C**, Normalized sarcomeric fluorescence amplitude is shown for the green and far-red channels with fitted exponential decay and accumulation curves (dotted lines) and calculated half-lives (bold dot and number; n=11, 22, 26, and 13 cells for ACTN2, MYOM1, MYBPC3, and MYL2, respectively, each from N=3 independent experiments). **D**, Normalized sarcomeric fluorescence intensity is shown in the far-red channel for unbleached (light red) and bleached (light blue) myofibrils, showing similar rates of accumulation. **E**, Normalized sarcomeric fluorescence intensity is shown in the green channel, showing exponential decay in the unbleached myofibril (light green) and no recovery in the bleached myofibril (light blue), except for some recovery in MYL2.

Downloaded from http://ahajournals.org by on December 16, 2024

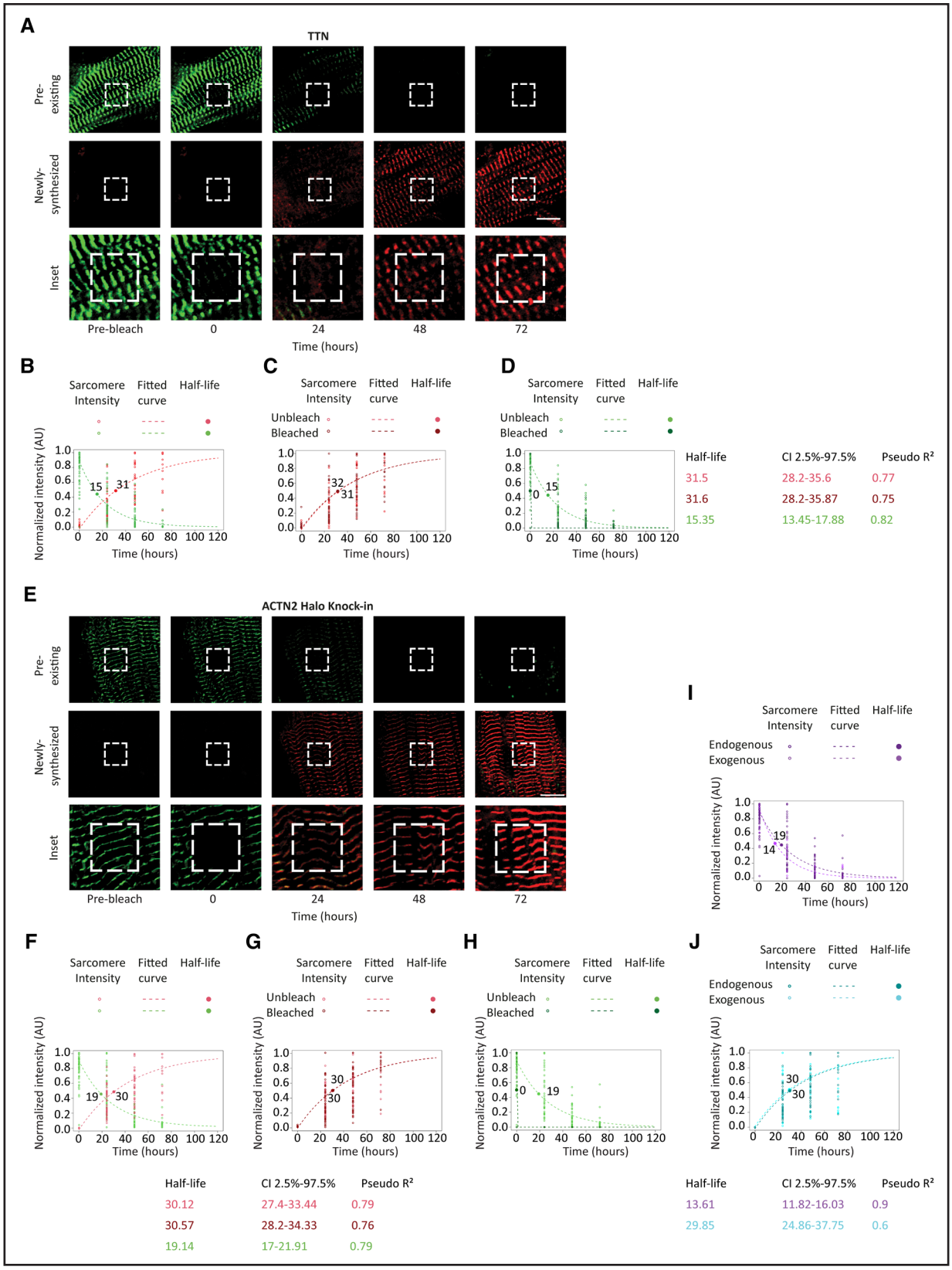

Figure 2. Imaging turnover of the endogenous sarcomeric proteins TTN and ACTN2.
A, Representative time-lapse images of neonatal mouse ventricular cardiomyocytes from Halo-tagged TTN knock-in mice in the green (top), far-red (middle), and magnified merged inset (bottom), before the photobleaching, immediately after (0), and at 24, 48, and 72 hours, showing gradual replacement of preexisting TTN proteins (green) with newly synthesized ones (far-red). The dashed white square is the photobleached field. It is gradually filling with new far-red–labeled proteins but not with green-labeled ones. Scale bar: 30 µm. **B**, Normalized sarcomeric (*Continued*)

Downloaded from http://ahajournals.org by on December 16, 2024

Sarcomere Protein Degradation Is Independent of Protein Age and Controls Turnover Rate

We wanted to determine whether young and old proteins in the sarcomere are turned over at the same rate. We used MYOM1-Halo that has a strong signal and expressed it in NRVM using an adenoviral vector. After 48 hours, we incubated the cells with the Oregon Green ligand and then with the JF-635 ligand for an additional 48 hours, allowing us to follow the degradation of 2 main populations of sarcomeric proteins in the myocytes: older proteins labeled green and newer proteins labeled far-red over the next 72 hours (Figure 3A). A computational simulation of this protocol showed that age-dependent degradation should result in a large difference between the half-lives of old and new proteins (Figure S7A through S7D). We observed a gradual decline in the sarcomeric signal intensity for both the old and the new proteins (Figure 3B). We fitted the signal data to an exponential decay function (Figure S8A) and found similar rates of decay and a similar half-life for both the old and new MYOM1 proteins (Figure 3C and 3D). We also used an alternative protocol, ensuring that the youngest green-labeled proteins are at least 12 hours older than the oldest red-labeled ones (Figure S8B). Following these cells for 72 hours showed that the half-lives of the old and new MYOM1 proteins were similar as well (Figure S8C through S8E). These results support a stochastic model where all proteins have the same likelihood of being removed and degraded, regardless of how old they are.

Both calpain and proteasomal proteases are responsible for the degradation of sarcomeric proteins.[26] However, it is not known if the proteolytic activity of these enzymes is required for the removal of proteins from the sarcomeric complex or whether sarcomeric proteins can detach intact from the complex and are only degraded later. To differentiate between these 2 hypotheses, we used MG-132, which is capable of inhibiting both calpains and the proteasome.[27] We expressed ACTN2-Halo in NRVMs and measured the half-life of ACTN2-Halo with or without incubation with MG-132. The inhibition of proteases by MG-132 resulted in a marked delay in the removal of existing green-labeled ACTN2-Halo proteins from the sarcomeric structure with a significant increase in the ACTN2 sarcomeric half-life (Figure 3E through 3G). We validated the effect of MG-132 using a Western blot (Figure S9A) and used it to estimate the half-life of endogenous ACTN2 (Figure S9B and S9C). We performed the same imaging analysis with endogenous TTN and similarly observed a marked delay in the removal of existing TTN (Figure 3H through 3J). To specifically assess the role of calpains, we used the calpain-1 inhibitor ALLN (N-acetyl-leucyl-leucyl-norleucinal). We show that, like with MG-132, the inhibition by ALLN results in a significant delay in the removal of endogenous Halo-TTN from the sarcomere with an increased half-life (Figure S9D through S9F). This delayed turnover indicates that proteolytic activity is required for the removal of sarcomeric proteins such as ACTN2 and TTN from the sarcomeric structure.

Earlier, we posited that sarcomeric proteins are translated abundantly, accompanied by swift proteasomal degradation of any unincorporated proteins.[28] In agreement with this proposal, we found that newly translated ACTN2-Halo proteins accumulated outside the Z-line structure following proteolytic blockade. By 72 hours, multiple aggregates composed predominantly of newly translated far-red–labeled proteins were observed (Figure 3K; Figure S10A). Interestingly, we also detected several discreet large aggregates predominantly made of older green-labeled ACTN2-Halo proteins (Figure 3K). Unlike ACTN2-Halo, which was overexpressed in these experiments, the Halo-TTN is an endogenous protein. Large aggregates composed of newly translated far-red–labeled Halo-TTN were observed between the myofibrils after proteolytic blockade, but these accumulations were not as dense as those of ACTN2-Halo (Figure 3I; Figure S10B).

Imaging Protein Turnover In Vivo Using Viral Vectors

To image and quantify the turnover of sarcomeric proteins in vivo in the adult mouse heart, we transduced neonatal mice with AAV vectors encoding TPM1-Halo

Figure 2 Continued. fluorescence amplitude is shown for the green and far-red channels with fitted exponential decay and accumulation curves (dotted lines) and calculated half-lives (bold dot and number). n=41 cells from N=3 independent experiments. **C**, Normalized sarcomeric fluorescence intensity is shown in the far-red channel for unbleached (light red) and bleached (dark red) myofibrils, showing a similar degree of accumulation. **D**, Normalized sarcomeric fluorescence intensity is shown in the green channel, showing exponential decay in the unbleached myofibril (light green) and no recovery in the bleached myofibril (dark green). **E**, Representative time-lapse images of NMVM after HITI knock-in of HaloTag to the *Actn2* locus using the same protocol as in (**A**), showing gradual replacement of existing endogenous ACTN2 proteins (green) with newly translated ones (far-red). The photobleached field is gradually filling with new far-red–labeled proteins but not with green-labeled ones. **F** through **H**, Quantification and calculation of assembly and degradation half-lives for endogenous ACTN2 as in (**B** through **D**) n=44 cells from N=3 independent experiments. **I** and **J**, Comparison of turnover rates of endogenous knocked-in ACTN2-Halo to exogenous virally expressed ACTN2-Halo in NMVMs. Normalized sarcomeric fluorescence amplitude is shown for the green (**I**) and far-red (**J**) channels with fitted exponential decay and accumulation curves (dotted lines) and calculated half-lives (bold dot and number). The deep and light purple dots and lines in (**I**) show the degradation of endogenous and exogenous virally expressed ACTN2 from the green channel, respectively. The deep and light cyan dots and lines in (**J**) show the accumulation of endogenous and exogenous virally expressed ACTN2 from the far-red. n=44 endogenous HITI cardiomyocytes and n=22 exogenous virally transduced cardiomyocytes, each from N=3 independent experiments. ACTN2, α-actinin 2; HITI, homology-independent targeted integration; NMVM, neonatal mice ventricular cardiomyocyte; and TTN, titin.

Downloaded from http://ahajournals.org by on December 16, 2024

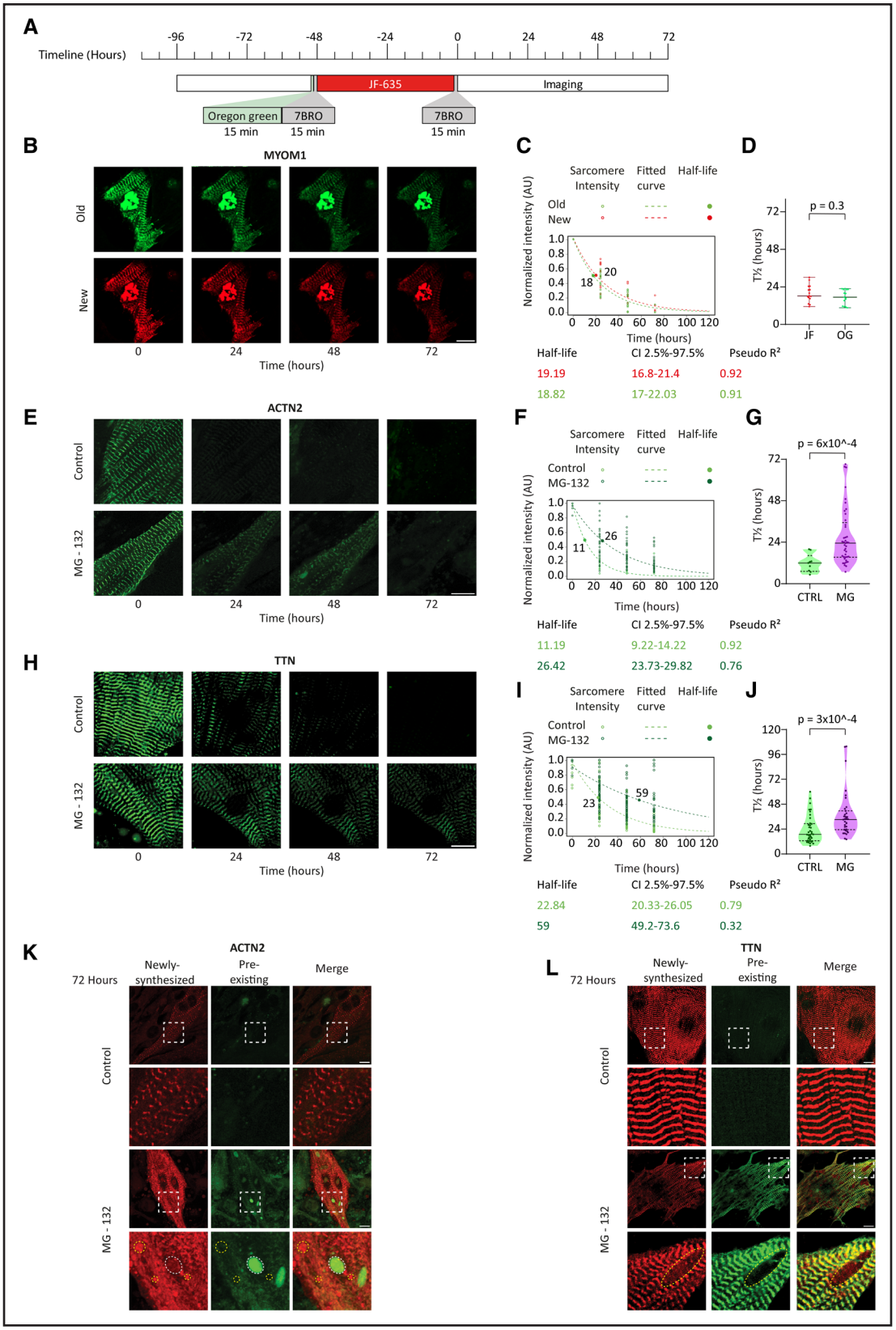

Figure 3. Degradation is independent of protein age and requires proteases.
A, Degradation experiment timeline: Cardiomyocytes expressing MYOM1-Halo for 48 hours were incubated with the OG and then with the JF-635 Halo-ligand for an additional 48 hours and imaged in a time lapse of 72 hours. **B**, Representative images of cardiomyocytes at 0, 24, 48, and 72 hours show a gradual decline of the sarcomeric signal in both the green and far-red channels. Scale bar: 10.25 µm. **C** and **D**, Quantification of normalized sarcomeric fluorescence intensity in the green (OG) and far-red (JF) channels (**C**), showing the half-lives of newer and (*Continued*)

Downloaded from http://ahajournals.org by on December 16, 2024

or ACTN2-Halo full-length proteins. After waiting for the mice to reach the age of 4 months, we injected the nonfluorescent blocker 7BRO intravenously and intraperitoneally to ensure saturation of all the available HaloTags. We then waited either 3 hours, 3 days, or 7 days and intravenously delivered the fluorescent JF-525 (Janelia Fluor-525) HaloTag ligand. For TPM1-Halo, we also included a 1-day group. To measure the maximal possible labeling intensity, we also delivered Halo-ligand JF-525 to mice that did not receive the 7BRO blocker. In addition to the 3 hours group, we included another negative control group of mice that received the ligands but not the AAVs encoding for Halo-tagged proteins (Figure 4A). We harvested the hearts 40 minutes after the injection of the JF-525 Halo-ligand and sectioned. Low and high magnification images of cardiac sections showed background signal in the 3 hours negative control group (Figure 4B through 4E); the sarcomeric fluorescence signal was increased by 3 days, and more so after 7 days, and was highest in the no 7BRO cardiomyocytes. In the latter, it was evident that the transduction rates are high, albeit with some cell-to-cell variability. As we did in the cultured cardiomyocytes, we drew a region of interest along the myofibril in individual cardiomyocytes in the sections (Figure 4D through 4G) and calculated the median amplitude of the sarcomeric signal (Figure 4H and 4I). We fitted the data to a 1 minus exponential decay function and estimated the half-lives of ACTN2 and TPM1 to be 270 and 108 hours, respectively (Figure 4J and 4K). We found that the measured half-life of ACTN2 in vivo was ≈10-fold longer than in cultured neonatal cardiomyocytes, indicating a slowing of the turnover as cardiomyocytes matured.

Imaging Endogenous TTN Turnover In Vivo

We again used the TTN-Halo knock-in mice[23] and used a similar labeling approach to the one we used in the AAV-transduced mice. Here, we included more labeling time points, with injection of Halo-ligand JF-525 at 3, 7, and 14 days after the injection of the blocker (Figure 5A). We also added Halo-ligand JF-525 to the cardiac sections to ensure complete labeling. Representative images of the sections and of cells at low and high magnification showed no sarcomeric signal with injection after 3 hours, indicating blockade was complete, and an increasing sarcomeric signal at 3, 7, and 14 days (Figure 5B through 5D). The group that did not receive the nonfluorescent blocker showed maximal signal intensity. We used the same analysis approach we used for the AAV-transduced hearts. We drew a region of interest along the myofibril axis on individual cardiomyocytes (Figure 5D) and used an automated tool to calculate the median amplitude of the sarcomeric signal along the line (Figure 5E). We fitted the data to a 1 minus exponential decay function and estimated the half-life of endogenous TTN to be 159 hours (Figure 5F). This number is more than 5-fold longer than the turnover of TTN in cultured NMVMs, indicating a marked slowdown in TTN turnover after maturation. To measure the half-life of TTN in neonatal mice in vivo, we injected 1-day-old pups with the 7BRO blocker and harvested the hearts after 3 hours, 1, 3, 7, or 10 days with labeling of Halo-TTN with JF-525. We also included Halo-tagged TTN mice that did not receive the 7BRO blocker to measure the maximal possible labeling intensity (Figure S11A). In neonatal mice, TTN has a half-life of 86 hours, implying a turnover rate shorter than that of adult mice (Figure S11B through S11F).

We next aimed to analyze the Halo-tagged TTN mice after induction of cardiac hypertrophy. Administration of phenylephrine (PE) activates α1-adrenergic receptors and is known to stimulate cardiomyocyte protein synthesis in mice.[29] We used a PE injection protocol in the Halo-tagged TTN mice and verified that it indeed resulted in a significant increase in normalized heart weight, indicative of hypertrophy (Figure S12A). We asked whether hypertrophy and an increased protein synthesis would also result in increased turnover rate of TTN. We therefore included groups of mice in which we injected PE in parallel with the Halo-ligand pulse-chase protocol (Figure 5B through 5F; Figure S12B). The average maximal labeling intensity observed in the group that did not receive the 7BRO blocker was higher in the PE-treated mice, but

Figure 3 Continued. older proteins in individual cardiomyocytes did not differ (**D**, n=15 cells, N=2 independent experiments, Wilcoxon matched-pairs signed-ranks test). **E**, Representative time-lapse images of NRVMs expressing ACTN2-Halo incubated with (bottom) or without (top) MG-132 at 0, 24, 48, and 72 hours in the green channel show that inhibition of proteases by MG-132 resulted in a marked delay in the removal of existing OG-labeled proteins from the sarcomere. Scale bar: 10 µm. **F** and **G**, Quantification of normalized sarcomeric fluorescence intensity for control (light green, Ctrl) and MG-132–treated cardiomyocytes (dark green; **F**) show much longer half-lives of ACTN2-Halo in MG-132–treated cardiomyocytes than in control cardiomyocytes (**G**; n=9, 41 cells for control and MG-132, respectively, each from N=3 independent experiments, Mann-Whitney *U* test). **H** though **J**, Similar analyses as in (**E** through **G**) in NMVMs from Halo-TTN knock-in mice show much longer half-lives of endogenous Halo-TTN in MG-132-treated cardiomyocytes relative to controls. Scale bar: 10 µm (n=37, 35 cells for control and MG-132, respectively, each from N=3 independent experiments, Mann-Whitney *U* test). **K**, Representative images of cardiomyocytes expressing ACTN2-Halo treated with control or MG-132 after 72 hours in the merged green and far-red channel with inset (dashed square) showing accumulation of newly translated far-red–labeled proteins outside the Z-line and multiple aggregates of newly translated (yellow dotted circle) proteins and some aggregates of old proteins (white dotted circle). Scale bar: 10 µm. **L**, Representative images of cardiomyocytes with knock-in Halo-TTN treated with control or MG-132 after 72 hours in the merged green and far-red channels with inset (dashed square) showing aggregates composed of newly translated far-red–labeled proteins (yellow dotted circle) that displace the myofibrils. Scale bar: 10 µm. 7BRO indicates 7-bromoheptanol; ACTN2, α-actinin 2; JF, JF-635; MG, MG-132; NMVM, neonatal mice ventricular cardiomyocyte; OG, Oregon Green; and TTN, titin.

Downloaded from http://ahajournals.org by on December 16, 2024

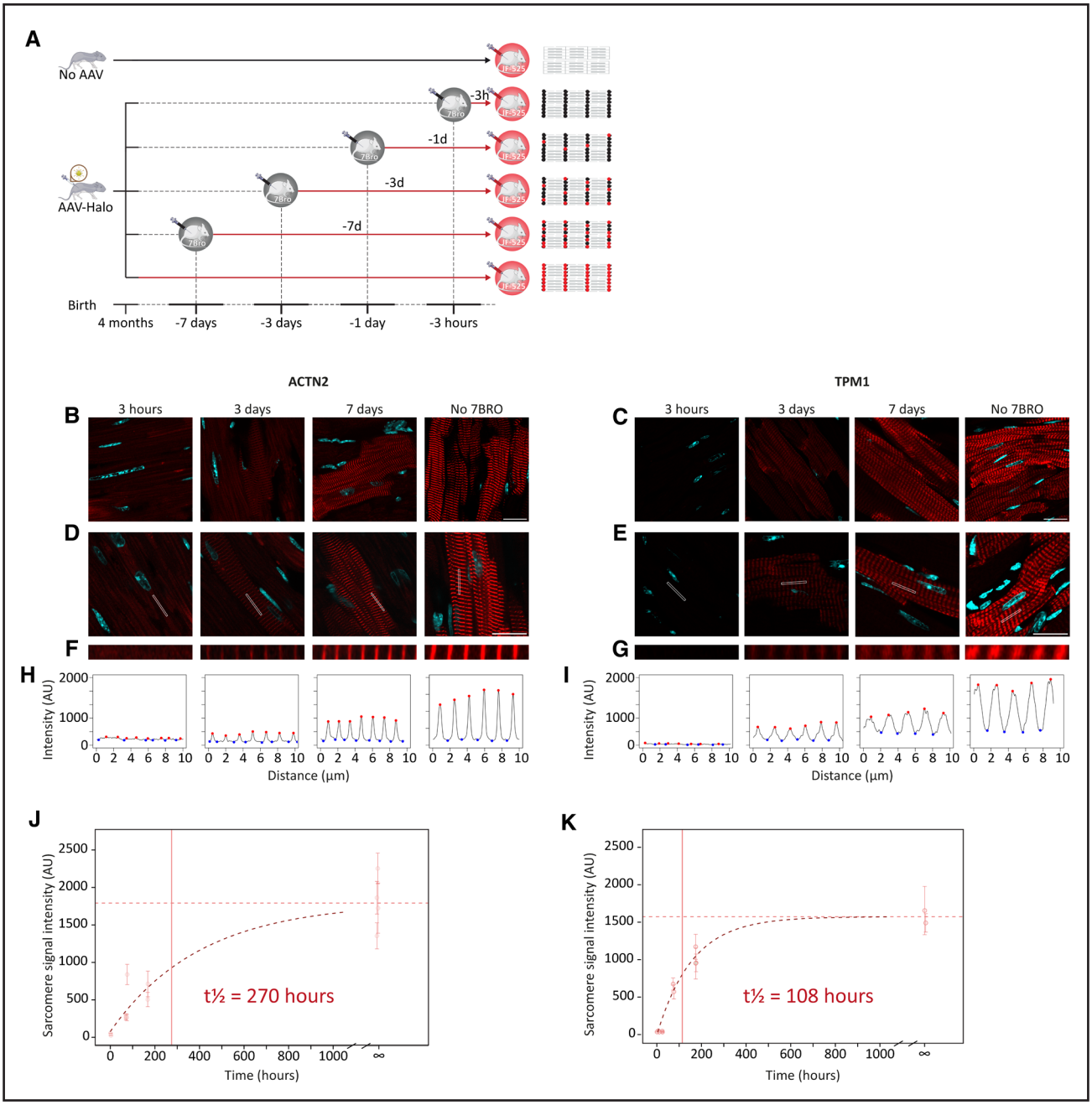

Figure 4. Imaging of sarcomeric protein turnover in vivo.

A, Neonatal mice were divided into 6 groups. In the "No AAV" group, no AAV injection was administered, while in the other 5 groups, mice received AAV9 encoding for either ACTN2-Halo or TPM1-Halo. In adulthood, all groups received an intravenous injection of the JF-525 Halo-ligand, and their hearts were harvested for analysis after 40 minutes. Mice in the No AAV and the No 7BRO groups did not receive intravenous injection of the nonfluorescent blocker ligand 7BRO, while mice in the other groups received 7BRO 3 hours or 1, 3, or 7 days before the JF-525 ligand injection, respectively. **B** through **G**, Representative images of the 4 groups of mice transduced with ACTN2-Halo (left) or TPM1-Halo (right) at low magnification (**B** and **C**, scale bar: 15 µm) and higher magnification (**D** and **E**, scale bar: 10 µm). A 10 µm region of interest along the myofibril is marked in (**D** and **E**) by a white rectangle and is shown at higher magnification in (**F** and **G**). **H** and **I**, Analysis of the JF-525 signal amplitude along the bar shown in (**F** and **G**). The red and blue dots are the local maxima and minima, identified automatically. **J** and **K**, The sarcomeric signal amplitude is plotted as a function of time after the 7BRO injection. Each dot represents the average of the sarcomere signal intensity from 1 mouse with ±SD whiskers. The No AAV groups were regarded as time 0, and the No 7BRO as the maximal possible signal, marked by a horizontal red dashed line. A fitted 1 minus exponential curve is shown as a dark red dashed line, and the calculated half-life is shown as a red vertical line. For ACTN2-Halo: n=10 cells/mouse, from n=2–4 mice/group (No AAV, n=2; 3 hours, n=2; 3 days, n=4; 7 days, n=2; No blocker, n=4). The estimated half-life of ACTN2 is 108.5±12.088 hours (SE). For TPM1-Halo: n=10 cells/mouse, from n=1-3 mice/group (No AAV, n=2; 3 hours, n=1; 1 day, n=2; 3 days, n=2; 7 days, n=3; No blocker, n=2). The estimated half-life of TPM1 is 270.3±77.171 hours (SE). R^2 was calculated to assess the goodness of fit, with values of 0.579 for ACTN2 and 0.936 for TPM1. 7BRO indicates 7-bromoheptanol; AAV, adeno-associated virus; ACTN2, α-actinin 2; JF-525, Janelia Fluor-525; and TPM1, tropomyosin 1.

Downloaded from http://ahajournals.org by on December 16, 2024

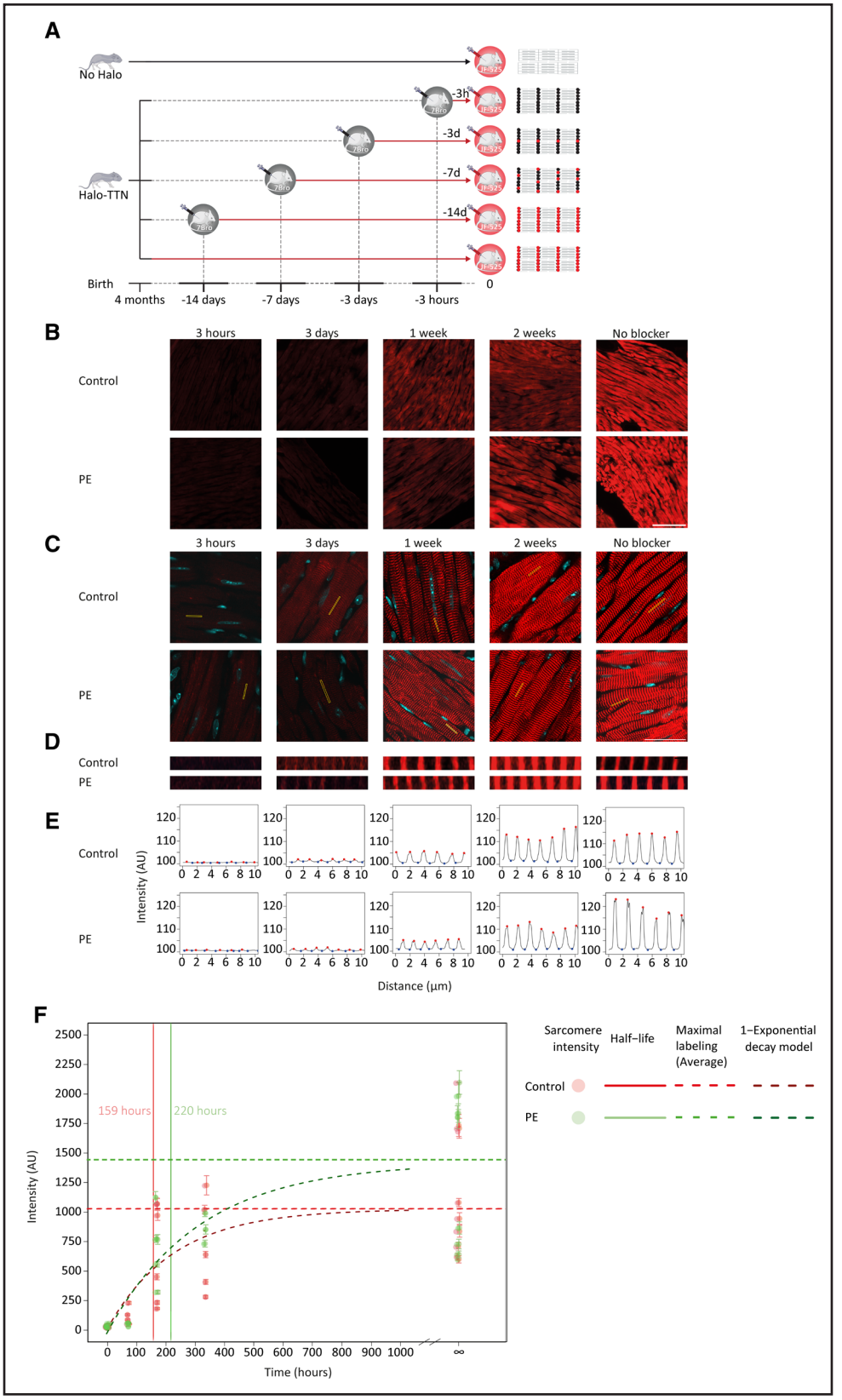

Figure 5. In vivo turnover of endogenous TTN in the normal heart and in hypertrophy.
A, Experiment design. Adult Halo-TTN knock-in mice received a nonfluorescent Halo-ligand (7BRO). After a chase period of 3 hours, 3 days, 1 week, or 2 weeks, mice received the JF-525 ligand, and the hearts were harvested. To measure the maximal labeling, 1 group of HaloTag-TTN knock-in mice received the fluorescent ligand without the 7BRO blocker. A negative control group of wild-type (WT) mice also received the fluorescent ligand without the 7BRO blocker. **B** through **D**, Representative images of cardiac sections from the different groups for (*Continued*)

Downloaded from http://ahajournals.org by on December 16, 2024

the difference was not statistically significant. Accordingly, the half-life calculated for the PE group was slightly longer than in the control group (220 versus 159 hours), but the difference was not statistically significant. These data suggest that the turnover of titin is not significantly accelerated in hypertrophy. The use of global fitting for analysis of the data showed similar half-life values (Figure S13).

Finally, we analyzed the turnover rates in different regions of the heart. We chose the left ventricular free wall, the interventricular septum, and the right ventricular free wall as representative regions and measured the half-life of TTN in each of them. Our analysis showed that TTN is turned over in different regions of the heart at similar rates (Figure S14).

DISCUSSION

Here, we developed a pulse-chase approach based on the ability of Halo-tagged proteins to covalently bind fluorescent ligands. This approach allowed us to visualize preexisting and newly translated proteins, measure their assembly and degradation rates, and uncover the mechanisms of sarcomeric maintenance. We showed that different sarcomeric proteins are uniformly turned over at similar rates, that turnover is slower in vivo in adult mice than in cultured neonatal cardiomyocytes or in neonatal mice, and that the turnover of the giant protein TTN is uniform throughout the heart. We challenged the prevailing protein pool hypothesis for sarcomeric maintenance and found that assembly is unidirectional—newly translated proteins continuously and uniformly enter the structure, whereas already assembled proteins can only be removed and degraded. Furthermore, we demonstrated that older and newer sarcomeric proteins are not distinguished in the degradation process and that proteolytic extraction from the complex is a rate-limiting step in the turnover.

Proteomic approaches were used to measure the half-lives of cardiac proteins in cultured cells and in vivo.[8,30,31] However, proteomics averages the half-life of proteins over the entire heart tissue and cannot differentiate between cardiomyocytes and noncardiomyocytes. We did not measure the half-life of proteins per se but rather calculated the turnover inside the sarcomeric structure in cardiomyocytes. Nevertheless, for the giant protein TTN, the half-life of turnover measured by us, ≈6.7 to 9.2 days, was similar to the average 11.8-day half-life calculated by proteomics.[30,32,33] Likewise, the half-lives we measured for ACTN2 and TPM1 of 11.3 and 4.5 days were comparable to the proteomics calculated half-lives of 11.4 and 7.15 days, respectively.[30] A hypertrophic stimulation did not alter the half-life of TTN, as was also observed with proteomics.[30]

It has been widely reported that sarcomeric proteins could be recycled.[11–13] These studies used fluorescence recovery after photobleaching with genetically encoded fluorophores, typically enhanced green fluorescent protein (eGFP) or YFP (yellow fluorescent protein), and extended the analysis time to many hours to show recovery. An inherent assumption of fluorescence recovery after photobleaching is that the transition between bright and dark states is irreversible. It is also possible, however, for fluorescent molecules to convert into a reversible dark state in a process called photoswitching. Several fluorescent molecules, including GFP, were shown to exhibit photoswitching,[34] and such reversible photoswitching may appear as mimicking diffusion. Indeed, 1 study that used fluorescently tagged TTN found extensive reversible photobleaching that accounted for most of the TTN fluorescence recovery.[35] Our experiments did not reveal any recovery of Oregon Green Halo-tagged sarcomeric proteins, even when we bleached at a submaximal level. This fluor is likely less prone to photoswitching, and unlike genetically encoded fluorophores, it does not need to fold or mature.

In contrast with assembly that is ordered, degradation appeared to be stochastic. Cardiomyocytes degrade old and new proteins at similar rates and likely cannot distinguish between them. We further showed that proteolytic extraction from the sarcomere is a rate-limiting step in the turnover of sarcomeric proteins. These findings also suggest that the degradation of sarcomeric proteins may be regulated. Furthermore, the proteolytic requirement for sarcomeric protein replacement we show supports the proteasome functional insufficiency hypothesis of heart failure.

Currently, no tools exist to visualize endogenous proteins in vivo in mice, so we relied on Halo-tagged proteins

Figure 5 Continued. control and phenylephrine (PE)-treated mice at low (**B**, scale bar: 100 µm) and high magnification (**C**, scale bar: 30 µm). The yellow box in (**C**) indicates a region of interest of ≈10 µm length used for quantification and is shown at high magnification in (**D**). **E**, Quantification of signals from (**D**). The local maxima and minima were identified automatically and marked in red and blue dots, respectively. **F**, Quantification of sarcomere labeling intensity from control mice (red) and mice that received PE (green). Each dot represents the mean sarcomere intensity of 10 cells from 10 different fields, acquired from a section of a single mouse heart. The error bars represent the SE. The no blocker control group data are indicated in infinity. The horizontal dashed line is the mean intensity in the no blocker positive control group and was used as a total protein reference in the model. The curved, dark dashed line is the fitting curve of the data to the 1 minus exponential decay model. The vertical solid lines indicate the half-life of the TTN protein calculated from the model for each group. Time is indicated in hours and intensity in arbitrary units (AU). Sample sizes were: n=10 cells/mouse, from n=3–8 mice/group (WT, n=4,3; 3 hours, n=4,3; 3 days, n=4,4; 7 days, n=6,5; 14 days, n=5,3; No blocker, n=8,7 mice for control and PE, respectively), from N=4 independent experiments (ANOVA between control and PE, after ranks transformation; P=0.52). The estimated half-life of TTN in the control group is 159±42 hours and 219.79±38.36 hours for the PE group. R^2 was calculated to assess the goodness of fit, with values of 0.514 for control and 0.731 for PE. 7BRO indicates 7-bromoheptanol; and TTN, titin.

Downloaded from http://ahajournals.org by on December 16, 2024

in cultured cardiomyocytes and in vivo. Tags can potentially interfere with the turnover of proteins; however, our analysis of endogenous and Halo-tagged α-actinin and comparisons with turnover rates from the literature showed similar half-lives.

In conclusion, we discovered mechanisms of sarcomere maintenance that could be useful for developing future treatments for genetic cardiomyopathies as well as for heart failure and hypertrophy. In particular, the requirements for enzymatic cleavage as a rate-limiting step in the process of replacement may be exploited to increase or delay the turnover of proteins in the sarcomeric structure. Finally, while we demonstrated how sarcomeres are maintained in cardiomyocytes, our findings likely apply to other heteromeric complexes in other cells.

ARTICLE INFORMATION

Received October 10, 2023; revision received June 26, 2024; accepted June 28, 2024.

Affiliations

The Rappaport Family Institute and the Bruce Rappaport Faculty of Medicine, Technion – Israel Institute of Technology, Haifa, Israel (G.D., I.E., L.H.-C., T.M., I.K.). Institute of Experimental Pharmacology and Toxicology, University Medical Center Hamburg-Eppendorf, Germany (M.P., L.C.). German Centre for Cardiovascular Research, partner site Hamburg/Kiel/Lübeck, Germany (M.P., L.C.); Now with Department of Cardiology, Boston Children's Hospital, Harvard Medical School, Boston, MA (M.P.). Centro Nacional de Investigaciones Cardiovasculares, Madrid, Spain (M.R.P., J.A.-C.). Institute of Physiology II, University of Munster, Germany (W.A.L.).

Acknowledgments

The authors wish to thank the Biomedical Core Facility at the Faculty of Medicine, Technion, the Technion Genomic Center, and the Pre-Clinical Research Authority at the Technion. The authors wish to thank Luke D. Lavis and Jonathan B. Grimm, Janelia Research Campus, Howard Hughes Medical Institute, Ashburn, VA, for their generosity in providing the Janelia Fluor HaloTag ligands.

Sources of Funding

Funding for this study was provided by the Israel Science Foundation (grant number: 1385/20) to I. Kehat and by the Fondation Leducq Research grant number 20CVD01 to I. Kehat and L. Carrier. W.A. Linke acknowledges funding from the German Research Foundation (grant number: Li690/14-1). The Centro Nacional de Investigaciones Cardiovasculares (CNIC) is supported by the Instituto de Salud Carlos III, the Ministerio de Ciencia e Innovación (MCIN; MCIN/AEI/10.13039/501100011033), and the Pro CNIC Foundation and is a Severo Ochoa Center of Excellence (grant number CEX2020-001041-S funded by MCIN).

Disclosures

None.

Supplemental Material

Supplementary Methods 36,37
Figures S1–S14
Uncut Gel Blots
Major Resources Table
ARRIVE Checklist

REFERENCES

1. Goehring NW, Hyman AA. Organelle growth control through limiting pools of cytoplasmic components. *Curr Biol.* 2012;22:R330–R339. doi: 10.1016/j.cub.2012.03.046
2. Kortazar D, Fanarraga ML, Carranza G, Bellido J, Villegas JC, Avila J, Zabala JC. Role of cofactors B (TBCB) and E (TBCE) in tubulin heterodimer dissociation. *Exp Cell Res.* 2007;313:425–436. doi: 10.1016/j.yexcr.2006.09.002
3. Kotila T, Wioland H, Enkavi G, Kogan K, Vattulainen I, Jégou A, Romet-Lemonne G, Lappalainen P. Mechanism of synergistic actin filament pointed end depolymerization by cyclase-associated protein and cofilin. *Nat Commun.* 2019;10:5320. doi: 10.1038/s41467-019-13213-2
4. Marsh JA, Teichmann SA. Structure, dynamics, assembly, and evolution of protein complexes. *Annu Rev Biochem.* 2015;84:551–575. doi: 10.1146/annurev-biochem-060614-034142
5. Gallastegui N, Groll M. The 26S proteasome: assembly and function of a destructive machine. *Trends Biochem Sci.* 2010;35:634–642. doi: 10.1016/j.tibs.2010.05.005
6. Taggart JC, Zauber H, Selbach M, Li GW, McShane E. Keeping the proportions of protein complex components in check. *Cell Syst.* 2020;10:125–132. doi: 10.1016/j.cels.2020.01.004
7. Yin Z, Ren J, Guo W. Sarcomeric protein isoform transitions in cardiac muscle: a journey to heart failure. *Biochim Biophys Acta.* 2015;1852:47–52. doi: 10.1016/j.bbadis.2014.11.003
8. Martin A. Turnover of cardiac troponin subunits. Kinetic evidence for a precursor pool of troponin-I. *J Biol Chem.* 1981;256:964–968. PMID: 7451483
9. Hamdani N, Borbély A, Veenstra SPGR, Kooij V, Vrydag W, Zaremba R, Dos Remedios C, Niessen HWM, Michel MC, Paulus WJ, et al. More severe cellular phenotype in human idiopathic dilated cardiomyopathy compared to ischemic heart disease. *J Muscle Res Cell Motil.* 2010;31:289–301. doi: 10.1007/s10974-010-9231-8
10. Chen CY, Caporizzo MA, Bedi K, Vite A, Bogush AI, Robison P, Heffler JG, Salomon AK, Kelly NA, Babu A, et al. Suppression of detyrosinated microtubules improves cardiomyocyte function in human heart failure. *Nat Med.* 2018;24:1225–1233. doi: 10.1038/s41591-018-0046-2
11. Sanger JM, Sanger JW. The dynamic Z bands of striated muscle cells. *Sci Signal.* 2008;1:pe37. doi: 10.1126/scisignal.132pe37
12. Islam M, Diwan A, Mani K. Come together: protein assemblies, aggregates and the sarcostat at the heart of cardiac myocyte homeostasis. *Front Physiol.* 2020;11:586. doi: 10.3389/fphys.2020.00586
13. Rudolph F, Hüttemeister J, da Silva Lopes K, Jüttner R, Yu L, Bergmann N, Friedrich D, Preibisch S, Wagner E, Lehnart SE, et al. Resolving titin's lifecycle and the spatial organization of protein turnover in mouse cardiomyocytes. *Proc Natl Acad Sci USA.* 2019;116:25126–25136. doi: 10.1073/pnas.1904385116
14. Skwarek-Maruszewska A, Hotulainen P, Mattila PK, Lappalainen P. Contractility-dependent actin dynamics in cardiomyocyte sarcomeres. *J Cell Sci.* 2009;122:2119–2126. doi: 10.1242/jcs.046805
15. Suzuki H, Komiyama M, Konno A, Shimada Y. Exchangeability of actin in cardiac myocytes and fibroblasts as determined by fluorescence photobleaching recovery. *Tissue Cell.* 1998;30:274–280. doi: 10.1016/s0040-8166(98)80076-1
16. Wang J, Sanger JM, Kang S, Thurston H, Abbott LZ, Dube DK, Sanger JW. Ectopic expression and dynamics of TPM1α and TPM1κ in myofibrils of avian myotubes. *Cell Motil Cytoskeleton.* 2007;64:767–776. doi: 10.1002/cm.20221
17. da Silva Lopes K, Pietas A, Radke MH, Gotthardt M. Titin visualization in real time reveals an unexpected level of mobility within and between sarcomeres. *J Cell Biol.* 2011;193:785–798. doi: 10.1083/jcb.201010099
18. Auerbach D, Bantle S, Keller S, Hinderling V, Leu M, Ehler E, Perriard JC. Different domains of the M-band protein myomesin are involved in myosin binding and M-band targeting. *Mol Biol Cell.* 1999;10:1297–1308. doi: 10.1091/mbc.10.5.1297
19. Welikson RE, Fischman DA. The C-terminal IgI domains of myosin-binding proteins C and H (MyBP-C and MyBP-H) are both necessary and sufficient for the intracellular crosslinking of sarcomeric myosin in transfected non-muscle cells. *J Cell Sci.* 2002;115:3517–3526. doi: 10.1242/jcs.115.17.3517
20. Los GV, Encell LP, McDougall MG, Hartzell DD, Karassina N, Zimprich C, Wood MG, Learish R, Ohana RF, Urh M, et al. HaloTag: a novel protein labeling technology for cell imaging and protein analysis. *ACS Chem Biol.* 2008;3:373–382. doi: 10.1021/cb800025k
21. Merrill RA, Song J, Kephart RA, Klomp AJ, Noack CE, Strack S. A robust and economical pulse-chase protocol to measure the turnover of HaloTag fusion proteins. *J Biol Chem.* 2019;294:16164–16171. doi: 10.1074/jbc.RA119.010596
22. Deo C, Abdelfattah AS, Bhargava HK, Berro AJ, Falco N, Farrants H, Moeyaert B, Chupanova M, Lavis LD, Schreiter ER. The HaloTag as a general scaffold for far-red tunable chemigenetic indicators. *Nat Chem Biol.* 2021;17:718–723. doi: 10.1038/s41589-021-00775-w
23. Rivas-Pardo JA, Li Y, Mártonfalvi Z, Tapia-Rojo R, Unger A, Fernández-Trasancos A, Herrero-Galán E, Velázquez-Carreras D,

Downloaded from http://ahajournals.org by on December 16, 2024

Fernández JM, Linke WA, et al. A HaloTag-TEV genetic cassette for mechanical phenotyping of proteins from tissues. *Nat Commun*. 2020;11:2060. doi: 10.1038/s41467-020-15465-9
24. Suzuki K, Izpisua Belmonte JC. In vivo genome editing via the HITI method as a tool for gene therapy. *J Hum Genet*. 2018;63:157–164. doi: 10.1038/s10038-017-0352-4
25. Platt RJ, Chen S, Zhou Y, Yim MJ, Swiech L, Kempton HR, Dahlman JE, Parnas O, Eisenhaure TM, Jovanovic M, et al. CRISPR-Cas9 knockin mice for genome editing and cancer modeling. *Cell*. 2014;159:440–455. doi: 10.1016/j.cell.2014.09.014
26. Martin TG, Kirk JA. Under construction: the dynamic assembly, maintenance, and degradation of the cardiac sarcomere. *J Mol Cell Cardiol*. 2020;148:89–102. doi: 10.1016/j.yjmcc.2020.08.018
27. Kitagawa S. Experimental manipulation of calpain activity in vitro. In: *Methods in Molecular Biology*. Humana Press Inc. 2019:209–218.
28. Lewis YE, Moskovitz A, Mutlak M, Heineke J, Caspi LH, Kehat I. Localization of transcripts, translation, and degradation for spatiotemporal sarcomere maintenance. *J Mol Cell Cardiol*. 2018;116:16–28. doi: 10.1016/j.yjmcc.2018.01.012
29. Scarborough EA, Uchida K, Vogel M, Erlitzki N, Iyer M, Phyo SA, Bogush A, Kehat I, Prosser BL. Microtubules orchestrate local translation to enable cardiac growth. *Nat Commun*. 2021;12:1547. doi: 10.1038/s41467-021-21685-4
30. Lau E, Cao Q, Ng DCM, Bleakley BJ, Dincer TU, Bot BM, Wang D, Liem DA, Lam MPY, Ge J, et al. A large dataset of protein dynamics in the mammalian heart proteome. *Sci Data*. 2016;3:160015. doi: 10.1038/sdata.2016.15
31. Wood NB, Kelly CM, O'Leary TS, Martin JL, Previs MJ. Cardiac myosin filaments are maintained by stochastic protein replacement. *Mol Cell Proteomics*. 2022;21:100274. doi: 10.1016/j.mcpro.2022.100274
32. Fornasiero EF, Mandad S, Wildhagen H, Alevra M, Rammner B, Keihani S, Opazo F, Urban I, Ischebeck T, Sakib MS, et al. Precisely measured protein lifetimes in the mouse brain reveal differences across tissues and subcellular fractions. *Nat Commun*. 2018;9:4230. doi: 10.1038/s41467-018-06519-0
33. Swist S, Unger A, Li Y, Vöge A, von Frieling-Salewsky M, Skärlén A, Cacciani N, Braun T, Larsson L, Linke WA. Maintenance of sarcomeric integrity in adult muscle cells crucially depends on Z-disc anchored titin. *Nat Commun*. 2020;11:4479. doi: 10.1038/s41467-020-18131-2
34. Mueller F, Morisaki T, Mazza D, McNally JG. Minimizing the impact of photoswitching of fluorescent proteins on FRAP analysis. *Biophys J*. 2012;102:1656–1665. doi: 10.1016/j.bpj.2012.02.029
35. Cadar AG, Feaster TK, Bersell KR, Wang L, Hong TT, Balsamo JA, Zhang Z, Chun YW, Nam YJ, Gotthardt M, Knollmann BC, Roden DM, Lim CC, Hong CC. Real-time visualization of titin dynamics reveals extensive reversible photobleaching in human induced pluripotent stem cell-derived cardiomyocytes. *Am J Physiol Cell Physiol*. 2020;318:C163–C173. doi: 10.1152/ajpcell.00107.2019
36. Golan-Lagziel T, Lewis YE, Shkedi O, Douvdevany G, Caspi LH, Kehat I. Analysis of rat cardiac myocytes and fibroblasts identifies combinatorial enhancer organization and transcription factor families. *J Mol Cell Cardiol*. 2018;116:91–105. doi: 10.1016/j.yjmcc.2018.02.003
37. Schlesinger-Laufer M, Douvdevany G, Haimovich-Caspi L, Zohar Y, Shofty R, Kehat I. A simple adeno-associated virus-based approach for the generation of cardiac genetic models in rats. *F1000Research*. 2020;9:ISF–1441. doi: 10.12688/f1000research.27675.1

Downloaded from http://ahajournals.org by on December 16, 2024